J Mater Sci (2006) 41:7696–7703
DOI 10.1007/s10853-006-0966-y

Coincidence-site lattices as rational approximants to irrational twins

S. Ranganathan · A. K. Srivastava · E. A. Lord

Received: 3 September 2006 / Accepted: 11 September 2006 / Published online: 31 October 2006

Abstract It is well known that sequences of crystals with Mackay icosahedral motif and increasing lattice parameters exist converging to the icosahedral quasicrystal in the limit. They are known as rational approximants. It has also been demonstrated that it is possible to create icosahedral symmetry by irrational twins involving five variants by 72° rotations around an irrational axis [τ 1 0] or an irrational angle of 44.48° around a rotation axis [1 1 1]. These twinned crystals do not share a coincidence site lattice. In this paper, it is demonstrated that the above twinning relationship arises in the limit of a sequence of coincidence site lattices starting with the cubic twins with $\Sigma = 3$ and extending through $\Sigma = 7, 19, 49, 129, 337, \ldots, \infty$ created by rotation around [1 1 1] axis. It is also noted that the boundaries of higher CSL values ($\Sigma > 7$) are composed of a combination of structural units from $\Sigma = 3$ and $\Sigma = 7$ boundaries.

Introduction

Interest in purely geometrical ideas of interfaces received an impetus over four decades ago with the application of the coincidence site lattice (CSL) concept to the atomic configuration at grain boundaries [1, 2]. Even though the geometrical approach does not predict energy, it has been useful in a comparison of results with atomistic calculations and high resolution electron microscopic observations [3–5]. The literature of CSL theory is now very extensive and the CSL concept plays a fundamental role in understanding the nature of grain boundaries in polycrystalline materials, and the phenomenon of twinning [6].

The first evidence of irrational twinning of cubic crystals of α-AlMnSi structure was reported by Bendersky et al. [7] in rapidly solidified Al–Mn–Fe–Si system. They have shown that the five variants of cubic crystals (symmetry $Pm\bar{3}$) rotated 72° about an irrational axis [1 τ 0] result in icosahderal point group symmetry ($m\bar{3}\bar{5}$). It was pointed out that the orientation relationship between the crystals is such that the icosahedral motifs in all the crystals are parallel. The cubic axes undergo a 5-fold rotation about an irrational axis $\langle 1\ \tau\ 0\rangle$, but only five orientations occur among hundreds of crystals. These twins are distinctly different from Pauling's [8] icosatwins model which are generated by a rotation around $\langle 1\ 1\ 0\rangle$ by 70.53° corresponding to $\Sigma = 3$. The important point to emphasize is that although the twin lattice is equivalent to coincidence site lattice (CSL) of bicrystals in grain boundary literature [9], the irrational twin lattices do not fit the twinning laws discussed in classical crystallography [10]. Subsequently, these irrational twins were reported by various authors [11–18] in different Al-transition metal alloy systems with Si or Ge additions. Bendersky and Cahn [19] have recently described a tiling pattern involving pentagons, originated by Albrecht Dürer, as an illuminating simple two-dimensional example of

S. Ranganathan (✉) · E. A. Lord
Department of Metallurgy, Centre for Advanced Study, Indian Institute of Science, Bangalore 560012, India
e-mail: rangu@met.iisc.ernet.in

A. K. Srivastava
Division of Materials Characterization, National Physical Laboratory, Electron Microscope Section, Dr. K.S. Krishnan Road, New Delhi 110012, India

twinning of a two-dimensional periodic pattern that can be irrationally twinned, and have related it to observed grain orientations in $Al_{13}Fe_4$ and α-Al–Mn–Fe–Si, and cited other examples in the literature.

The present work aims to demonstrate that these cases, in which no CSL exists ("$\Sigma = \infty$") can be considered as limiting cases involving of sequences of CSLs of decreasing density.

An important advance occurred with the realization that an arbitrary grain boundary can be thought of as a combination of structural units from favored grain boundaries [3, 4]. The structural unit model (SUM) developed by Sutton and Vitek [4] has been successfully utilized to elucidate the sequence of fundamental units at the grain boundaries. A structural unit is defined as a group of atoms arranged in a characteristic configuration [20–22]. The favored boundaries are composed of a uniform array of a single type of structural unit, whilst those between them are composed of combinations of structural units from adjoining favored boundaries. An instructive example is the $\Sigma = 99$ boundary in aluminum arising from a rotation of 89.5° around [1 1 0] axis [23]. Mills [24] has explained that, on the basis of the structural unit model, the $\Sigma = 99$ (557) boundary should be composed of a mixture of the structural units of the $\Sigma = 3$ (1 1 1) 70.53° coherent twin boundary and the $\Sigma = 3$ (1 1 2) 109.5° incoherent twin boundary. Paidar and Erhart [25] developed a decomposition scheme into structural units to analyze the $\Sigma = 9$ and $\Sigma = 11$ asymmetrical boundaries in the fcc lattice.

The advent of quasicrystals has had an important repercussion on our ideas concerning the structure of irrational interfaces. The concepts of quasicrystals, rational approximants and irrational interfaces are briefly reviewed below.

In 1984, Shechtman and coworkers [26] reported the occurrence of the icosahedral quasicrystalline phase in a rapidly solidified Al–Mn alloy. The icosahedral phase shows 5-fold, 3-fold and 2-fold rotational symmetry with 3 dimensional quasiperiodicity. The point group of this phase in reciprocal space displays $m\bar{3}\bar{5}$ symmetry. Soon after the discovery of the icosahedral phase, Chattopadhyay et al. [27] and Bendersky et al. [28], reported the decagonal phase having 10/mmm symmetry in reciprocal space with 2-dimensional quasiperiodicity.

The rational approximant structures (RAS) are large unit cell structures whose diffraction patterns closely resemble those from quasicrystals [29]. They can be derived by projection from the 6-dimensional space, if τ is replaced by a rational approximant p/q wher q and p are successive terms in the Fibonacci sequence 1, 1, 2, 3, 5, 8, 13, … Some examples of RAS with their different p/q values are listed in Table 1. Their pseudo 5-fold axes corresponding to true 5-fold [τ 1 0] axis in the quasicrystals have also been indicated.

Table 1 Rational approximant structures, the order of approximant, pseudo 5-fold axes and planes

N	P/q	Example	[A5]	(A5)
1	1/0	Al–Cu–Ru	3 2 0	2 1 0
2	1/1	α-Al–Mn–Si T–Mg–Zn–Al Ti–Mn–Si	5 3 0	3 2 0
3	2/1	Al–Pd–Mn	8 5 0	5 3 0
4	3/2	Mg–Zn–Al Ga–Mg–Zn Ti–Zn–Ni	13 8 0	8 5 0
5	5/3	Ti–Zn–Ni	21 13 0	13 8 0

Chattopadhyay et al. [30] reported that the τ phases occurring in Al–Cu–Ni alloys can be interpreted as one dimensional quasicrystals. They can be obtained by a projection method along axes $[qq\bar{p}]$ where p/q is a Fibonacci approximant to τ [31]. Among the RAS, the cubic α-AlMnSi [32] and T-MgAlZn [33] are the most commonly occurring RAS for icosahedral quasicrystals. The phase α-AlMnSi, 1/1 RAS, has a cubic structure of two-shell Mackay icosahedra with a cluster of 54 atoms [34]. All icosahedra are parallel in this structure and the nearest neighbors are linked along their common three fold axis. The lattice has symmetry $m\bar{3}m$ and the motif has symmetry $m\bar{3}\bar{5}$. Thus the structure has symmetry $m\bar{3}$, governed by the intersection of the lattice and motif symmetry. It is significant to note that $m\bar{3}\bar{5}$ and $m\bar{3}m$ are not related as group–subgroup.

The advent of quasicrystals inspired Rivier [35] to forge a link between quasiperiodicity and grain boundaries. This was extended by Sutton [36, 37] to show that irrational tilt grain boundaries in ordinary crystalline materials display one dimensional quasiperiodic arrangement of structural units. Gratias and Thalal [38] emphasized the importance of higher dimensional approach to demonstrate that the geometric description of quasiperiodicity links the general and coincidence lattice grain boundaries.

The test for these theories is provided by the irrational interfaces observed by Bendersky et al. [7]. The multiple twinning of cubic crystals leading to the icosahedral symmetry in reciprocal space could be considered as a special case of CSL $\Sigma = \infty$. The twin boundaries have a low energy, so that they can accommodate the translational displacement in a way similar to quasicrystals.

Evidence for twinning in Al–Mn–Cr–Si [15, 16] and Al–Fe–V–Si [13, 18] alloys has been observed. Icosahedral quasicrystalline grains in Al–Fe–V–Si were surrounded by the crystalline aggregate of α-Al(Fe,V)Si. The crystalline particles are embedded in α-Al matrix. The composite symmetry generated by the crystalline variants in both the alloys was icosahedral.

Axis/angle pair description for CSLs for rotation around [1 1 1]

Ranganathan's generating function [2] was used to calculate all the values of Σ and corresponding angles of misorientation, θ, for specific axes of misorientation, *UVW*, for cubic crystals:

$$\Sigma = x^2 + Ny^2 \quad (1)$$

$$\tan(\theta/2) = y\sqrt{N}/x \quad (2)$$

where $N = U^2 + V^2 + W^2$ and x and y are coprime integers. The formula can be applied for non-cubic crystals, by replacing N by a different quadratic form in U, V and W, related to the nature of the lattice [39].

Table 2 CSLs for rotation on Ranganathan's generating function for *UVW* = 1 1 1

x	y	Σ	$\theta°$
3	1	3	60
5	1	7	38.21
8	2	19	46.83
13	3	49	43.57
21	5	129	44.82
34	8	337	44.35
τ^3	1	∞	44.48

By using the above equations, with x and y consecutive terms in the Fibonacci sequence (1, 1, 2, 3, 5, 8, 13, …), Σ takes the values 3, 7, 19, 49, 129, 337, …, ∞ for rotation axis [1 1 1]. Table 2 shows the different CSL values calculated and the corresponding θ values. For the lowest CSL, Σ = 3, the angle of misorientation is $\theta = 60°$ (arcsine $\sqrt{3}/2$). The angle of misorientation for Σ = 7 is $\theta = 38.21°$ (arcsine $5\sqrt{3}/14$). As the order of CSL increases, the θ value converges towards 44.48°. In the limiting case (i.e. Σ = ∞), the θ value associated with the [1 1 1] axis is 44.48° (arcsine $\tau\sqrt{3}/4$) corresponding to an irrational twin relationship in a cube and leads to an icosahedral symmetry operation [16]. This aspect will now be discussed in the context of 24 equivalent twinning operations for multiple twins, Σ = ∞.

Axis/angle pair description of CSL for Σ = ∞

For CSL Σ = ∞, 24 equivalent operations are obtained by combining 24 cube symmetry operations with an irrational axis of rotation $[0\,\bar{1}\,\tau]$ and an angle of rotation 72° (Table 3). These 24 equivalent twinning operations can be expressed as 7 different set of rotation axes with their angular misorientations [7].

All the five variants can be constructed by starting with one crystal and generating the remaining four by

Table 3 Axis-angle relationship of symmetry operations of a cube for a rotation of 72° about $[0\,\bar{1}\,\tau]$

S.No.	Axis	Rotation $\theta°$	Zone axis			Angle W°
	h k l		*u*	*v*	*w*	
1	0 0 1	90	$\bar{1}$	1	$\overline{\tau^3}$	154.76
2	0 0 1	180	$\bar{1}$	0	$\overline{\tau^2}$	120.00
3	0 0 1	270	1	1	1	44.48
4	0 1 0	90	$\bar{1}$	$\bar{1}$	$\bar{1}$	75.52
5	0 1 0	180	1	τ	0	144.00
6	0 1 0	270	$\bar{1}$	$\overline{2\tau-1}$	1	138.59
7	1 0 0	90	$\overline{\tau^3}$	τ^3	$\bar{1}$	110.21
8	1 0 0	180	τ^2	$\bar{\tau}$	$\bar{1}$	180.00
9	1 0 0	270	τ^3	$\bar{1}$	$\overline{\tau^3}$	110.21
10	1 1 0	180	$\overline{\tau^3}$	$\bar{1}$	1	154.76
11	1 0 1	180	$\overline{2\tau-1}$	1	$\bar{1}$	138.59
12	0 1 1	180	1	1	1	164.48
13	$\bar{1}$ 1 0	180	1	$\overline{\tau^3}$	$\bar{1}$	154.76
14	1 0 $\bar{1}$	180	1	$\bar{1}$	$\overline{2\tau-1}$	138.59
15	0 1 $\bar{1}$	180	$\bar{1}$	$\overline{\tau^3}$	τ^3	110.21
16	1 1 1	120	τ	0	1	144.00
17	1 1 1	240	$\overline{\tau^2}$	$\bar{1}$	0	120.00
18	1 1 $\bar{1}$	120	τ	0	$\bar{1}$	72.00
19	1 1 $\bar{1}$	240	$\bar{\tau}$	$\bar{1}$	τ^2	180.00
20	$\bar{1}$ 1 1	120	0	1	τ	144.00
21	$\bar{1}$ 1 1	240	0	$\overline{\tau^2}$	$\bar{1}$	120.00
22	1 $\bar{1}$ 1	120	$\bar{1}$	τ^2	$\bar{\tau}$	180.00
23	1 $\bar{1}$ 1	240	$\bar{1}$	τ	0	72.00

rotating four times about one of its $\langle 1\ \tau\ 0\rangle$ axes. At this stage first it is useful to designate the different variants as A, B, C, D, E. In this terminology A has been considered as the cubic crystal with 24 symmetry operations. B has one symmetry operation, $[0\,\bar{1}\,\tau]$ with 72° misorientation and the remaining 23 equivalent operations were obtained after combining $[0\,\bar{1}\,\tau]/72°$ with cubic symmetry operations, as reported in Table 3. Symmetry operations of crystal C, D and E can be obtained by combining $[0\,\bar{1}\,\tau]/144°$, $[0\,\bar{1}\,\tau]/216°$ and $[0\,\bar{1}\,\tau]/288°$, respectively with 24 cubic symmetry operations. The transformation matrices for the operation (a) $[0\,\bar{1}\,\tau]/72°$, (b) $[0\,\bar{1}\,\tau]/144°$, (c) $[0\,\bar{1}\,\tau]/216°$ and (d) $[0\,\bar{1}\,\tau]/288°$ are given below:

a. $\frac{1}{2}\begin{pmatrix} 1/\tau & -\tau & -1 \\ \tau & 1 & -1/\tau \\ 1 & -1/\tau & \tau \end{pmatrix}$

b. $\frac{1}{2}\begin{pmatrix} -\tau & -1 & -1/\tau \\ 1 & -1/\tau & -\tau \\ 1/\tau & -\tau & 1 \end{pmatrix}$

c. $\frac{1}{2}\begin{pmatrix} -\tau & 1 & 1/\tau \\ -1 & -1/\tau & -\tau \\ -1/\tau & -\tau & 1 \end{pmatrix}$

d. $\frac{1}{2}\begin{pmatrix} 1/\tau & \tau & 1 \\ -\tau & 1 & -1/\tau \\ -1 & -1/\tau & \tau \end{pmatrix}$

As an illustrative example the cubic lattice (having icosahedral motif) along a plane close to an irrational plane $[0\,\bar{1}\,\tau]$ has been displayed in Fig. 1. The rotation of the lattice by 72° leaves the motif invariant (Fig. 1b). Figure 1c shows the composite pattern after the five rotations about $[0\,\bar{1}\,\tau]$, leading to overall icoahedral symmetry.

Low order CSLs as rational approximants to Σ = ∞

Table 4 a–c lists the set of axis–angle pairs for CSLs Σ = 3, 7 and ∞ respectively. In the case of CSL Σ = 3, the 24 operations can be expressed as 5 different sets of axis–angle pairs and for CSL Σ = 7, the 24 operations

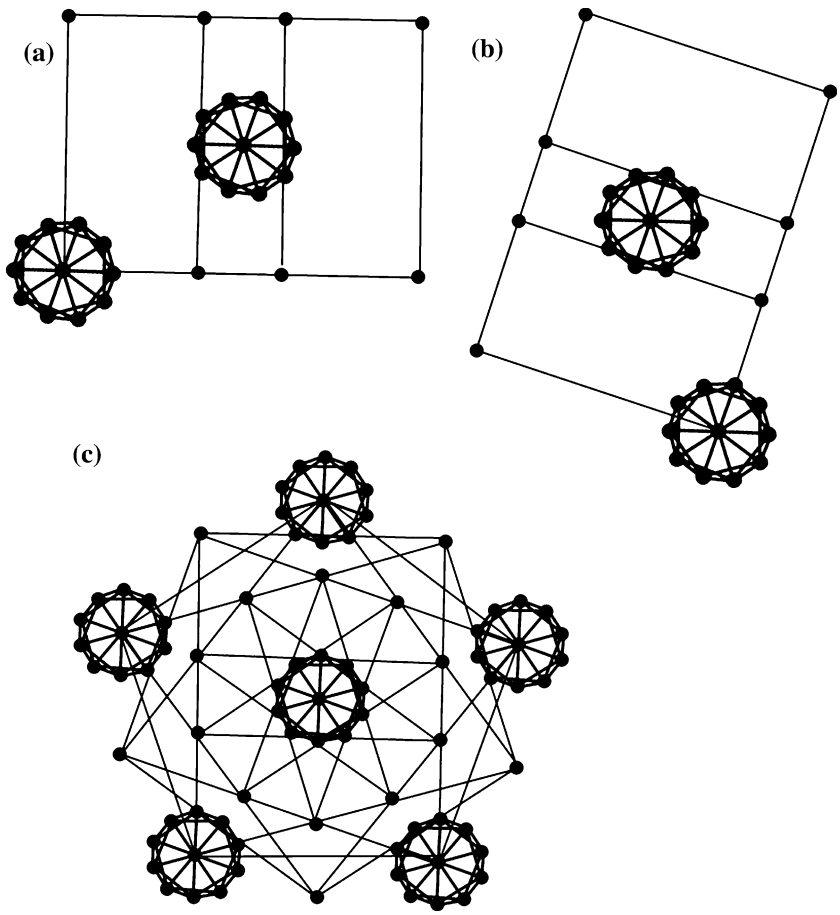

Fig. 1 (**a**) A plane close to $(0\,\bar{1}\,\tau)$ in a cubic lattice (having icosahedral motif), (**b**) plane after 72° rotation about $[0\,\bar{1}\,\tau]$ and (**c**) the icosahedral symmetry generated by the composite of all five variants

Table 4 Axis–angle relationship for CSLs (a) $\Sigma = 3$, (b) $\Sigma = 7$ and (c) $\Sigma = \infty$

Number	Type of axis	Angle of misorientation
(a) $\Sigma = 3$		
3	1 1 1	60, 180
3×2	1 1 0	70.53, 109.47
6	2 1 0	131.81
6	3 1 1	146.44
3	2 1 1	180
(b) $\Sigma = 7$		
3	1 1 1	38.21, 81.79, 158.21
3	2 1 0	73.40
3	3 2 0	149.00
3	3 3 1	110.92
3	3 1 0	115.38
3	2 1 1	135.38
3	5 1 1	158.21
3	3 2 1	180
(c) $\Sigma = \infty$		
3	1 1 1	44.48, 75.52, 164.48
6	$0\ \bar{1}\ \tau$	72, 144
3	$-\tau^3\ 1\ -\tau^3$	110.21
3	$1\ 0\ \tau^2$	120.00
3	$1\ 2\tau\ -1\ \bar{1}$	138.59
3	$1\ \bar{1}\ \tau^3$	154.76
3	$-\tau^2\ \tau\ 1$	180

can be expressed as 8 different set of zone axes and angles. There are 7 different sets of zone axes with the corresponding angle of misorientations for CSL $\Sigma = \infty$ (Table 4c). It was also found that there are 8 different sets of axis–angle pairs for CSLs $\Sigma = 19$, 49, 129 and 337. These different sets of axis–angle pairs for CSLs $\Sigma = 3$, 7, 19, 49, 129, 337 and ∞ are shown in Table 5. It is seen that the CSL $\Sigma = 3$, 7, 19, 49, 129, 337 and higher CSL values following this series can approximate the CSL $\Sigma = \infty$ axes very closely, even if CSL value is not very large. For example, the angular deviation from the 5-fold axis is about 1.47° for $\Sigma = 3$, 1.40° for $\Sigma = 7$, 0.41° for $\Sigma = 19$ and 0.17° for $\Sigma = 49$. For higher value CSLs the angular deviation is almost negligible and the axes are very close to the axes corresponding to $\Sigma = \infty$. It can be easily noticed that

Table 5 Set of axis–angle pairs for CSLs $\Sigma = 3$, 7, 19, 49, 129, 337 and ∞

Σ	[1 1 1] θ	2-fold $\tau^2\ \tau\ 1$	3-fold $\tau^2\ 1\ 0$	5-fold $\tau\ 1\ 0$	5-fold $\tau^2\ \tau\ 0$	2t–1 1 1	$\tau^3\ 1\ 1$	$\tau^3\ \tau^3\ 1$
3	1 1 1 60, 180	2 1 1 180	2 1 0 131.81	1 1 0 70.53	2 1 0 131.81	3 1 1 146.44	3 1 1 146.44	2 2 0 (= 1 1 0) 109.47
7	1 1 1 38.21, 81.79, 158.21	3 2 1 180	3 1 0 115.38	2 1 0 73.4	3 2 0 149	4 2 2 (= 2 1 1) 135.58	5 1 1 158.21	3 3 1 110.92
19	1 1 1 46.83, 73.17, 166.83	5 3 2 180	5 2 0 121.76	3 2 0 71.59	5 3 0 142.14	7 3 3 139.74	8 2 2 (= 4 1 1) 153.47	5 5 1 110.01
49	1 1 1 43.57, 76.43, 163.57	8 5 3 180	8 3 0 119.33	5 3 0 72.17	8 5 0 142.72	11 5 5 138.15	13 3 3 155.25	8 8 2 (= 4 4 1) 110.3
129	1 1 1 44.82, 75.18, 164.82	13 8 5 180	13 5 0 120.26	8 5 0 71.94	13 8 0 143.73	18 8 8 (= 9 4 4) 138.76	21 5 5 154.57	13 13 3 110.18
337	1 1 1 44.35, 75.65, 164.35	21 13 8 180	21 8 0 119.9	13 8 0 72.02	21 13 0 144.1	29 13 13 138.53	34 8 8 (= 17 4 4) 154.83	21 21 5 110.22
∞	1 1 1 44.82, 75.52, 164.48	$\tau^2\ \tau\ 1$ 180	$\tau^2\ 1\ 0$ 120	$\tau\ 1\ 0$ 72	$\tau^2\ \tau\ 0$ 144	$2\tau–1\ 1\ 1$ 138.59	$\tau^3\ 1\ 1$ 154.76	$\tau^3\ \tau^3\ 1$ 110.21

indices of each axis correspond to Fibonacci sequence and in the limit converge to τ or multiple of τ depending on the particular axis-angle pairs. It is also worth noting that the ratio of two consecutive Σ values from low order to higher order converges to 2.61 and in the limit the ratio is τ^2 (=2.618034…).

Figure 2 shows the stereograms displaying zone axes of $\Sigma = 3$, 7 and ∞. The pattern obtained by the misorientation $\Sigma = 3$ [1 1 1]/60° (Fig. 2a) shows hexagonal symmetry [9]. Figure 2b displays the misorientation $\Sigma = 7$ [1 1 1]/38.21° of rhombohedral symmetry [9]. The stereogram displaying the zone axes of $\Sigma = \infty$ [1 1 1]/44.48° is shown in Fig. 2c. The stereogram again shows the rhombohedral point group symmetry. The 7 different sets of axes belonging to the symmetry operations of an icosahedral point group can be seen (Fig. 2c). The 2-fold, 3-fold and 5-fold axes of the icosahedral symmetry are reflected as pseudo 5-fold [0 1 τ], pseudo 2-fold [1 τ^2 τ] and pseudo 3-fold [0 τ^2 1] vectors of the cube. The [1 1 1] direction of the cube also belongs to the 3-fold vectors of icosahedral point group. The vectors [1 1 τ^3], [1 τ^3 τ^3] and [1 2τ–1 1] with angle of rotations 154.76°, 110.21° and 138.59°, respectively are displayed in stereogram.

In the context of dichromatic patterns the misorientation [1 1 1]/60° and [1 1 1]/θ ($\theta \neq 60°$) yield the 6'/m'm'm and $\bar{3}$m' symmetry, respectively [9]. For operation [0 $\bar{1}$ τ]/72°, which means that a lattice originally coincident with the reference white lattice and with the same color is rotated by an angle 72° about [0 $\bar{1}$ τ] and subsequently undergoes color reversal from white to black. Therefore the operation [0 $\bar{1}$ τ]/72° could be represented as { [0 $\bar{1}$ τ]72°}', where prime denotes the color-reversing symmetry. All possible relative orientations of black and white lattices could be obtained in this way and therefore the composite symmetry in our case CSL $\Sigma = \infty$, leads to the symmetry of $\bar{3}$m'. The series of CSLs Σ = 7, 19, 49, … (Table 5) display the $\bar{3}$m' point symmetry.

The CSL approximants of $\Sigma = \infty$ mentioned in above sections can be demonstrated graphically. Ranganathan [2] has illustrated a method to demonstrate the CSLs on a given plane (*hkl*). Two perpendicular directions along *X* and *Y* axes are defined as [–($k^2 + l^2$), *hk*, *hl*] and [0 1 $\bar{k}$] with the axial ratio, $\sqrt{(h^2 + k^2 + l^2)}$. In Fig. 3, the (1 1 1) plane has been considered. The directions *X* and *Y* are [1 $\bar{1}$ 0] and [$\bar{1}$ $\bar{1}$ 2], respectively. The generating points for CSLs Σ = 3, 7, 19, 49, 129 and 337 are shown in the plot. An irrational line was drawn along $\theta/2 = 22.24°$. It is seen that the low value CSLs are located relatively away from the irrational line. As the CSL order increases the corresponding Σ values come closer to the irrational line. The higher order approximants are indistinguishable from the irrational line and the CSL points are almost overlapping the irrational line. This fact is already reflected in Table 5, where the angle of misorientations of the higher value CSLs, with the

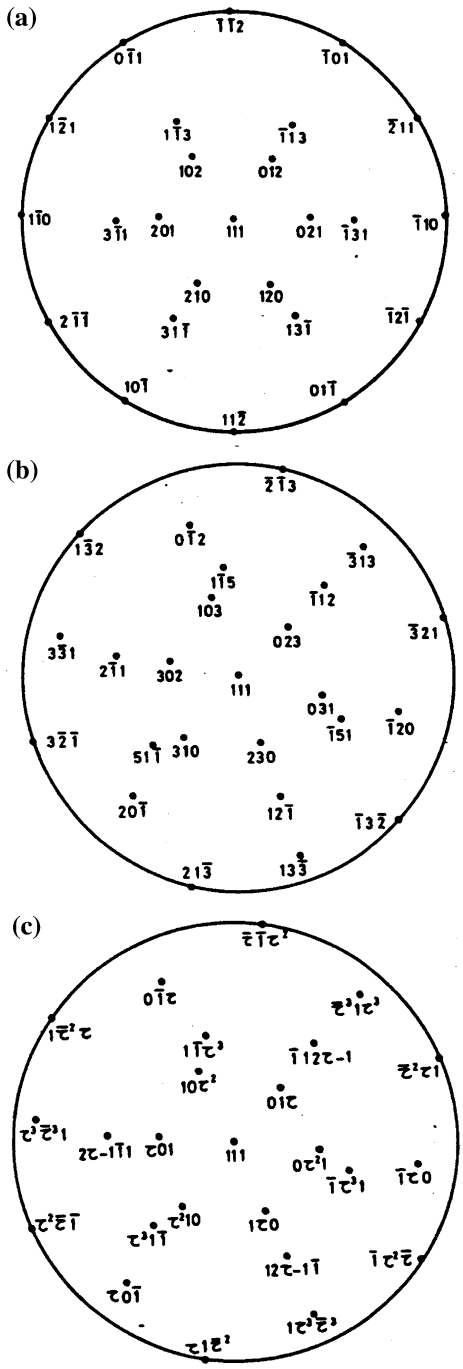

Fig. 2 Stereograms illustrating the axes for CSLs (**a**) $\Sigma = 3$, (**b**) $\Sigma = 7$ and (**c**) $\Sigma = \infty$

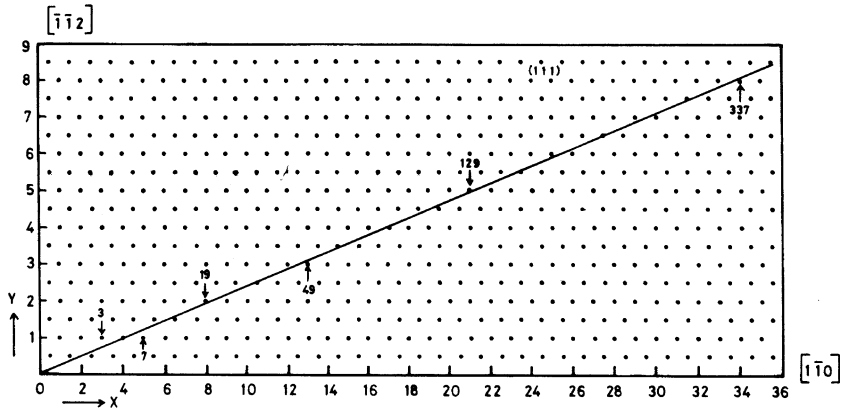

Fig. 3 Irrational line drawn along $\Sigma = \infty$ [1 1 1]/44.48°. Corresponding approximant CSLs are also plotted

corresponding axes, has very small deviation from the misorientations of the respective $\Sigma = \infty$ case.

Structural unit model

Sutton [36] has discussed the structure of irrational interfaces. The important point emphasized was that the interface displays long range order and local isomorphism and any irrational interface has a quasi-periodic structure. The structural unit model as developed by Sutton and Vitek [4] and Rivier [35] had definite rules for determining the sequence of structural units for arbitrarily large values of Σ. It was predicted that the CSLs $\Sigma > 7$ (Table 5) could be composed of $\Sigma = 3$ and $\Sigma = 7$ boundaries. If $\Sigma = 7$ [3 2 1]/180° boundary has a structural unit as P and $\Sigma = 3$ [2 1 1]/180° boundary has a structural unit as Q, the one complete period of the $\Sigma = 19$ [5 3 2]/180° boundary can be constructed based on the stacking of P and Q units, in the sequence of PQ (Table 6). For $\Sigma = 49$ [8 5 3]/180°, the P and Q units can be stacked in the sequence of PQP. Similarly for boundaries $\Sigma = 129$ [13 8 5]/180° and $\Sigma = 337$ [21 13 8]/180° units can be stacked in the sequence of PQPPQ and PQPPQPQP, respectively. The boundary $\Sigma = \infty$ [$\tau^2 \tau$ 1]/180° should be composed of a mixture of the structural units of P and Q, which are structural units of favored boundaries. The sequence achieved after stacking P and Q units yield the form—PQPPQPQPPQPPQ—in quasi-periodic order (Table 6).

Table 6 Coincidence-site lattices as Fibonacci series

CSLs Σ	P – 2 fold τ^2 τ 1	Stacking sequence
3	2 1 1	Q
7	3 2 1	P
19	5 3 2	P Q
49	8 5 3	P Q P
129	13 8 5	P Q P P Q
337	21 13 8	P Q P P Q P Q P
∞	τ^2 τ 1	… P Q P P Q P Q P P Q P P Q …(Quasiperiodic)

It was shown [35, 36] that the structural unit sequences could be obtained by the strip method. The strip method generates the same sequence of structural units as described by Sutton and Vitek [4]. Figure 4 illustrates the strip method for obtaining the sequences of units at the boundaries reported in Table 6. These boundary units are $\Sigma = 7$ [3 2 1]/180° and $\Sigma = 3$ [2 1 1]/180° as P and Q, respectively. The higher order CSLs ($\Sigma > 7$) are composed of mQ and nP units, where m and n are coprime numbers and $m < n$. In Fig. 4, the bold broken line lies within the strip and was obtained by sliding the elementary square along the line connecting the origin to (m, n). For example the boundary $\Sigma = 129$ [13 8 5]/180° composed of 3P and 2Q units, the structural unit tiles P and Q are the projection of the horizontal and vertical edges of the unit square and leads to the sequence PPQPQP (Fig. 4). Similarly the structural unit tiles P and Q for $\Sigma = 337$ [21 13 8]/180° leads to the sequence PPQPPQPQ.

A careful analysis of strip method shown for tiling the boundary with the structural units (Fig. 4) and Table 6 brings out some remarkable properties of the stacking sequence. The most important among these is the fact that the stacking sequence of P and Q units in the CSLs follows the same sequence known for the Fibonacci series. Table 6 shows the same inflation rules A $\rightarrow$ AB and B $\rightarrow$ A as discussed for the quasicrystal (Fig. 1). It has a great significance in understanding the geometry of the CSLs mentioned in Table 6. For each CSL, the repeat layer sequence can be generated by stacking P and Q in a Fibonacci and in the limit for $\Sigma = \infty$, the sequence converges to the quasiperiodic sequence.

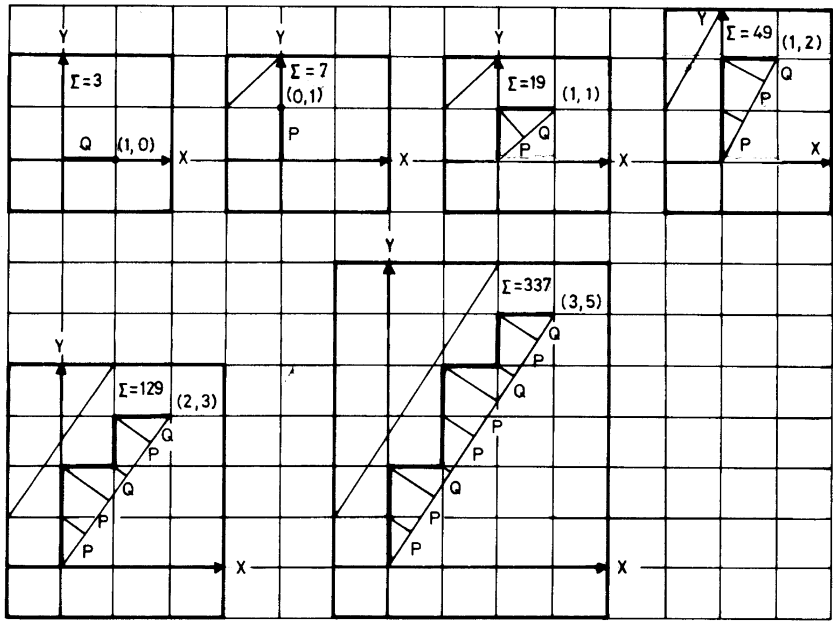

Fig. 4 Strip method for obtaining the sequence of units in a boundary composed of P and Q units

Conclusions

It has been demonstrated that in the limiting case the CSLs with $\Sigma = 3, 7, 19, 49, 129, 337, \ldots$ are the RAS of irrational twins. The composite symmetry generated by the irrational twinning operation of five cubic variants leads to the icosahedral point group. Except for the hexagonal symmetry shown by the bicrystal with $\Sigma = 3$, the bicrystals $\Sigma = 7, 19, 49, 129, 337, \ldots \infty$ display the rhombohedral symmetry. Higher order CSLs are composed of structural units from $\Sigma = 3$ and $\Sigma = 7$. It has been found that in the limit ($\Sigma = \infty$) the structural units $\Sigma = 3$ and $\Sigma = 7$ form a quasiperiodic sequence.

Acknowledgements The authors are grateful to Professor K. Chattopadhyay and Prof A L Mackay for valuable discussions. Figure 1 is after a discussion with Prof K F Kelton.

References

1. Brandon DG, Ralph B, Ranganathan S, Wald MS (1964) Acta Metall 12:813
2. Ranganathan S (1966) Acta Cryst 21:197
3. Bishop GH, Chalmers B (1968) Scr Metall 2:133
4. Sutton AP, Vitek V (1983) Philos Trans R Soc London Ser 309 A:1
5. Christian JW, Mahajan S (1995) Prog Mater Sci 39:1
6. Grimmer H, Nespolo M (2006) Z Kristallogr 221:28
7. Bendersky LA, Cahn JW, Gratias D (1989) Philos Mag 60B:837
8. Pauling L (1987) Phys Rev Lett 58:365
9. Pond RC, Bollmann W (1979) Philos Trans R Soc London Ser 292 A:449
10. Friedel G, in "Lecons de cristallographie" (Paris 1926, 2nd ed. 1964, Libraire Sci. A. Blanhard, Paris, 1964)
11. Koskenmaki DC, Chen HS, Rao KV (1986) Phys Rev 33 B:5328
12. Mandal RK, Sastry GVS, Lele S, Ranganathan S (1991) Scr Metall Mater 25:1477
13. Srivastava AK, Ranganathan S (1992) Scr Metall Mater 27:1241
14. Lalla NP, Tiwari RS, Srivastava ON (1992) J Mater Res 7:53
15. Singh A, Srivastava AK, Ranganathan S (1993) In: Krishnan KM (ed) Microstructure of materials. San Francisco Press, CA, p 152
16. Srivastava AK, Ranganathan S (1996) Acta Mater 44:2935
17. Srivastava AK, Ranganathan S (1997) Prog Cryst Growth Charact 34:251
18. Srivastava AK, Ranganathan S (2001) J Mater Res 16:2103
19. Bendersky LA, Cahn JM, J Mater Sci (2006, to be published)
20. Ashby MF, Spaepen F, Williams S (1978) Acta Metall 26:1647
21. Pond RC, Vitek V, Smith DA (1979) Acta Cryst 35A:689
22. Paidar V (1987) Acta Metall 35:2035
23. Dahmen U, Hetherington CJD, O'kee MA, Westmacott KH, Mills MJ, Daw MS, Vitek V (1990) Philos Mag Lett 62:327
24. Mills MJ (1993) Mater Sci Eng 166 A:35
25. Paidar V, Erhart J (1993) Interface Sci 1:115
26. Shechtman D, Blech I, Gratias D, Cahn JW (1984) Phys Rev Lett 53:1951
27. Chattopadhyay K, Ranganathan S, Subbanna GN, Thangaraj N (1985) Scr Metall 19:767
28. Bendersky LA (1985) Phys Rev Lett 55:1461
29. Goldman AI, Kelton KF (1993) Rev Mod Phys 65:213
30. Chattopadhyay K, Lele S, Thangaraj N, Ranganathan S (1987) Acta Metall 35:727
31. Lord E, Ranganathan S, Anandh Subrasmaniam (2002) Phil Mag 62:255
32. Cooper M, Robinson K (1966) Acta Cryst 20:614
33. Bergman G, Waugh JLT, Pauling L (1957) Acta Cryst 10:254
34. Mackay AL (1962) Acta Cryst 15:916
35. Rivier N (1986) J Phys (Paris) 47:C3-299
36. Sutton AP (1988) Acta Metall 36:1291
37. Sutton AP (1992) Prog Mater Sci 36:167
38. Gratias D, Thalal A (1988) Philos Mag Lett 57:63
39. Lord EA, Kristallogr Z (2006, to be published)